

Supplementary data

The Kemp elimination in membrane mimetic reaction media. Probing catalytic properties of cationic vesicles formed from a double-tailed amphiphile and linear long-tailed alcohols or alkyl pyranosides

Jaap E. Klijin and Jan B.F.N. Engberts

Ion Exchange Constant

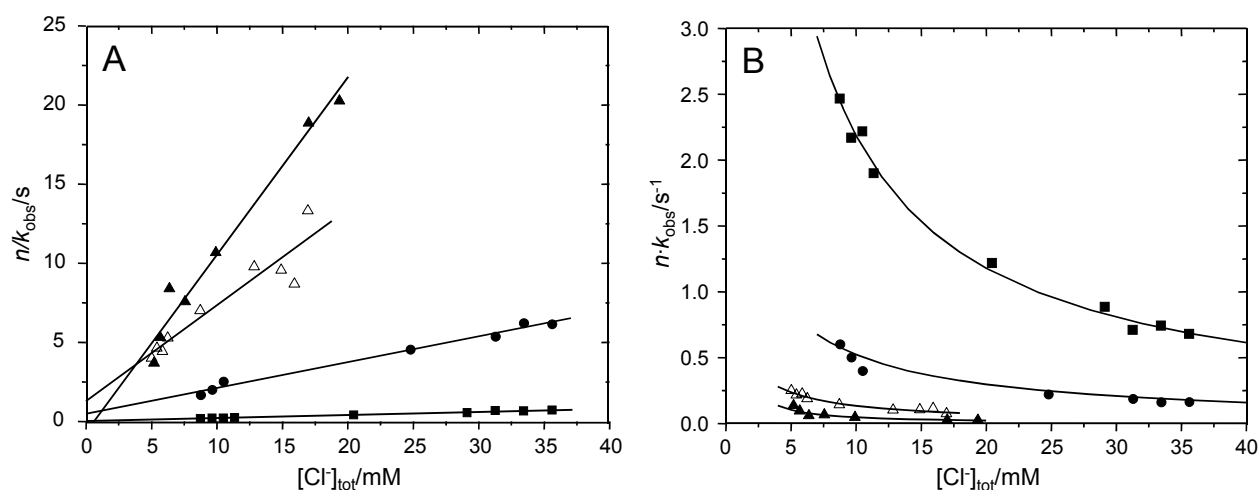


Figure 1. Linear (A) and non-linear (B) plots used to calculate K_{OH}^{Cl} . 20 mol% $C_{18}OH$ (\blacktriangle); 50 mol% $C_{18}OH$ (\triangle); 20 mol% $C_{18:1}OH$ (\bullet); 25 mol% $C_{12}Glu$ (\blacksquare). A: $n=1$, except $n=0.5$ for 50 mol% $C_{18}OH$. B: $n=1$, except $n=0.5$ for 25 mol% $C_{12}Glu$. Lines are best fits

Table 1. Values of K_{OH}^{Cl} obtained from linear and non-linear fits.

Solution	slope	intercept	$K_{OH}^{Cl\ a)}$	slope	intercept	$K_{OH}^{Cl\ b)}$
100% $C_{18}C_{18}^+$	477 ± 19	0.58 ± 0.06	1.8 ± 0.2	480 ± 21	0.62 ± 0.17	1.7 ± 0.5
20% $C_{18}OH$	600 ± 84	1.3 ± 0.9	1.1 ± 0.8	650 ± 190	0.97 ± 0.63	1.5 ± 1.1
50% $C_{18}OH$	2224 ± 167	-1.3 ± 3.7	-4 ± 12	2368 ± 523	-2.1 ± 1.8	-2.5 ± 2.2
20% $C_{18:1}OH$	162 ± 8	0.48 ± 0.04	0.75 ± 0.08	164 ± 43	0.46 ± 0.33	0.8 ± 0.6
26% $C_{12}Glu$	19.7 ± 0.9	0.0283 ± 0.0005	1.6 ± 0.1	19 ± 3	0.03 ± 0.02	1.3 ± 0.9

a) from linear fit b) from non-linear fit.

The ion exchange constant was calculated according to the literature.^{1,2} Negative values for $K_{\text{OH}^{\text{Cl}}}$ are physically impossible, values smaller than 1 are improbable. Therefore the average value of $K_{\text{OH}^{\text{Cl}}}$ was taken using the remaining fits. A value of 1.6 was calculated, independent of bilayer composition.

Vesicle Solubilisation by *n*-Dodecyl- β -Maltoside

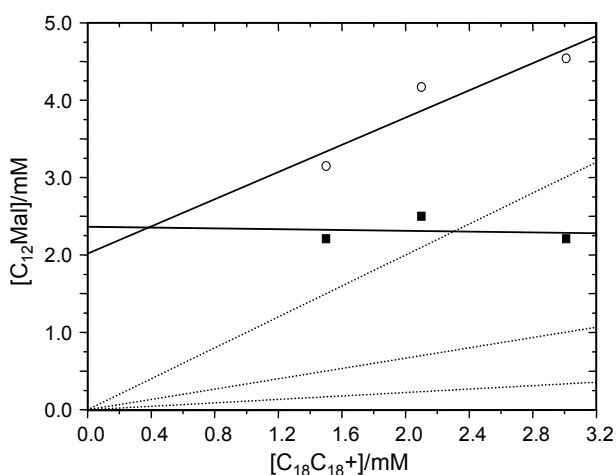


Figure 2. Diagram of vesicle solubilisation of $\text{C}_{18}\text{C}_{18}^+$ by C_{12}Mal . Solid lines are linear fits through the points of detergent saturated vesicles (■) and fully solubilised vesicles (○). Dotted lines represent solutions containing 10, 25 and 50 mol% C_{12}Mal .

Figure 2 shows the phase diagram of mixtures of $\text{C}_{18}\text{C}_{18}^+$ and C_{12}Mal in the presence of 2.25 mM NaOH. The mechanism of vesicle solubilisation is discussed in the literature.³⁻⁵ The phase diagram of mixtures of $\text{C}_{18}\text{C}_{18}^+$ and C_{12}Mal is only derived using a few data points, due to the odd behaviour of these detergent/amphiphile mixtures (vide infra). As a result the pattern is not very clear. For these reasons we refrain from a detailed interpretation at this stage. We only note that up to 3 mM of $\text{C}_{18}\text{C}_{18}^+$ about 2 mM C_{12}Mal is needed to saturate the membrane. The slope in the R_{sol} line is 0.88, which is rather small indicating that C_{12}Mal readily solubilises membranes of $\text{C}_{18}\text{C}_{18}^+$.

Dynamic Light Scattering of Solutions Containing *n*-Dodecyl- β -Maltoside

When the scattered intensity of these various solutions is considered (Figure 3A) it can be seen that above 25 mol% of C_{12}Mal the scattered intensity decreases.

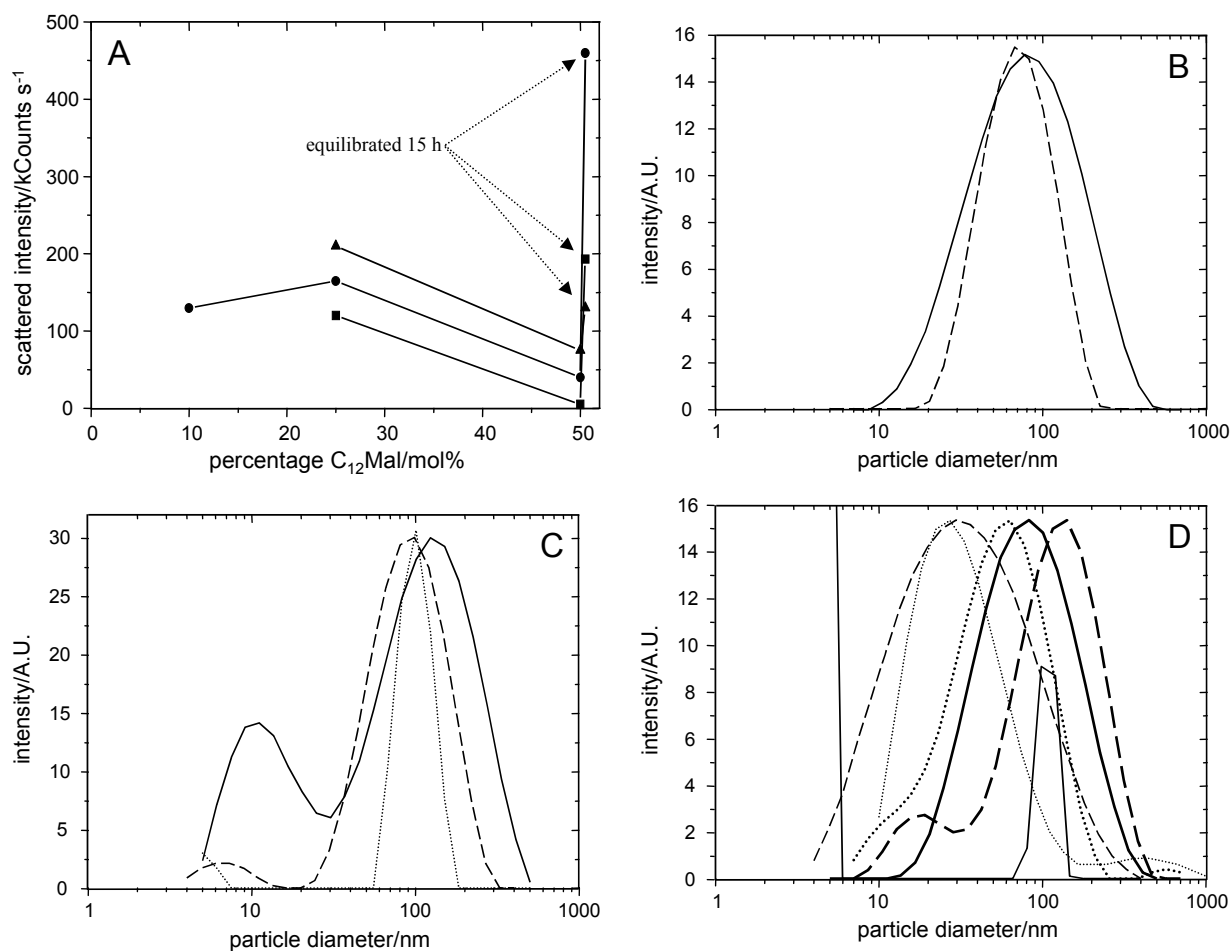


Figure 3. A: Plots of scattered intensity versus the mole percentage $C_{12}Mal$. No NaOH added (\blacksquare); 2.25 mM NaOH added (\bullet); diluted from a 30 mM stock solution after visual precipitation upon NaOH addition (\blacktriangle). B-D: Size distributions for 0 and 10 mol% $C_{12}Mal$ (B), 25 mol% $C_{12}Mal$ (C) and 50 mol% $C_{12}Mal$ (D). B: 2.25 mM NaOH. Solid line 0 mol% $C_{12}Mal$; dashed line 10 mol% $C_{12}Mal$. C+D: Solid line no NaOH added; dashed line 2.25 mM NaOH added; Dotted line from the visually precipitated solution. D: thin lines are from data directly after preparation; thick lines after 15 h equilibration.

DLS experiments were performed using solutions prepared in three different ways. In all three cases the vesicles were prepared as described above, but then NaOH was either not added, or added to a dilute vesicular solution, or to a concentrated vesicular solution, that was then shaken and subsequently diluted to the same concentration as the other solutions (0.5 mM $C_{18}C_{18}^+$).

The trend in the scattered intensity going from 25 mol% of $C_{12}Mal$ to 50 mol% $C_{12}Mal$ is the same for all three preparation methods. Upon equilibration over night the scattered intensity of the solution containing 50 mol% of $C_{12}Mal$ is increased for all three preparation methods. However, the absolute values are not the same.

The solution containing 10 mol% $C_{12}Mal$ (Figure 3B) show a monomodal distribution comparable to a solution without $C_{12}Mal$, except that the distribution is narrower. At 25 mol% of $C_{12}Mal$ in the absence of NaOH the distribution is bimodal (maximums at 10 nm and 125 nm), similar as in the presence of 2.25 mM NaOH. However, in the presence of NaOH the distribution is narrower. The peak on the small-size end of the graph is rather small, but this does not necessarily mean that the concentration of small particles (micelles) is small, since their scattering ability is rather poor. Vesicles from the precipitated solution show an even narrower distribution. At 50 mol% of $C_{12}Mal$ in the absence of NaOH there is peak

around 100 nm, but a large peak is showing up at sizes smaller than 5 nm. This observation is in agreement with the very low scattering intensity and indicates that the solution mainly consists of (worm-like) micelles and a few larger aggregates. Upon the addition of 2.25 mM NaOH smaller sized vesicles are formed (30 nm), but the distribution is rather broad (starting at 4 nm, and ending at 300 nm). Therefore we believe this solution is a broad mixture of large vesicles, worm-like micelles, and perhaps also spherical micelles. Over night, for all three solutions containing 50 mol% of $C_{12}Mal$ slightly larger vesicles are formed, as is also seen by large increases in the scattering intensity. At the small-particle side of the graph there is still a small peak indicating that there is still a large amount of small aggregates. However, at the large particle-side of the distribution small peaks are appearing indicating that also some large aggregates are formed. In fact, we visually observed on the bottom of the cuvet some precipitated vesicles, that were not solubilised upon shaking. In order to study the dynamics of the system, five solutions containing a fixed concentration $C_{18}C_{18}^+$ and varying amounts of $C_{12}Mal$ were prepared. A certain amount of a concentrated stock solution of $C_{12}Mal$ was added to a solution containing 2.1 mM $C_{18}C_{18}^+$ and 2.25 mM NaOH. Then they were left for 60 hours to equilibrate.

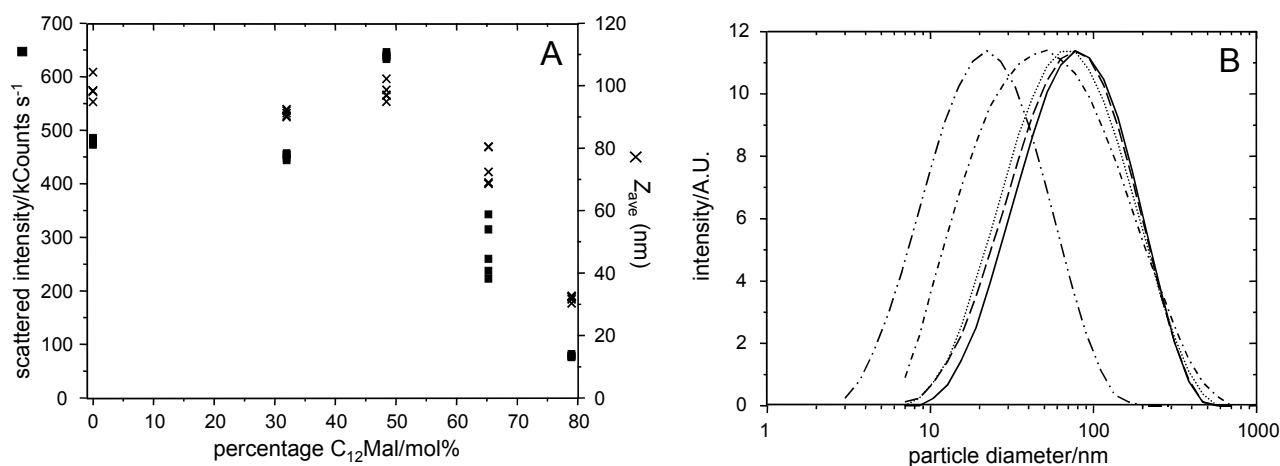


Figure 4. Plot of the scattered intensity and Z_{ave} (A) and size distribution (B) of vesicles formed from $C_{18}C_{18}^+$ and $C_{12}Mal$ at various mole fractions. A: scattered intensity (■) and Z_{ave} (×). B: $C_{12}Mal$: 0 mol% (solid line); 32 mol% (dashed line); 48 mol% (dotted line); 65 mol% (dash-dotted line) and 79 mol% (dash-double-dotted line).

In Figure 2 it can be seen that at 2.1 mM $C_{18}C_{18}^+$, saturation and solubilisation is supposed to occur around 50 mol% and 65 mol% of $C_{12}Mal$, respectively. In fact, at 50 mol% of $C_{12}Mal$ Z_{ave} and the scattered intensity reach a maximum. However, at 65 mol% still not all vesicles are solubilised into mixed micelles considering the scattered intensity. Even at 80 mol% of $C_{12}Mal$ complete solubilisation is not achieved. Apparently, turbidity experiments are not able to detect the remaining vesicles, or bilayer fragments.

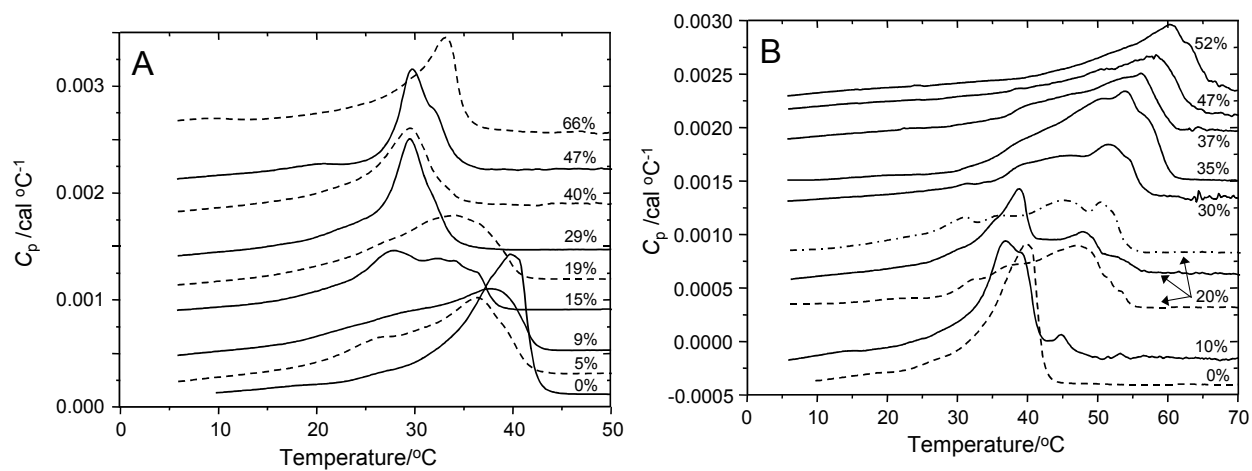
The size distributions shown in Figure 4B are in agreement with those shown in Figure 3. The most surprising feature is the absence of any indication of micelle formation in Figure 4B. The maximum in the size distribution decreases from around 80 nm to 20 nm, but there appears no peak in the spherical micellar region (5-6 nm).

A shift in the maximum, rather than the appearance of a peak around 5-6 nm has also been observed in the transition from vesicles to worm-like micelles to spherical micelles.^{6,7} Therefore, we propose that solubilisation by $C_{12}Mal$ proceeds via worm-like micelles.

We do not fully understand all the processes going on in solutions containing $C_{18}C_{18}^+$ and $C_{12}Mal$. Especially the addition of NaOH leads to substantial changes in the aggregates. It appears that upon addition of NaOH the vesicles tend to grow, but the extent and rate depend on the exact vesicle preparation procedure.

Differential Scanning Microcalorimetry

The DSC heating scans are shown for various mole percentages of the linear alcohols and alkyl pyranosides (Figure 5).



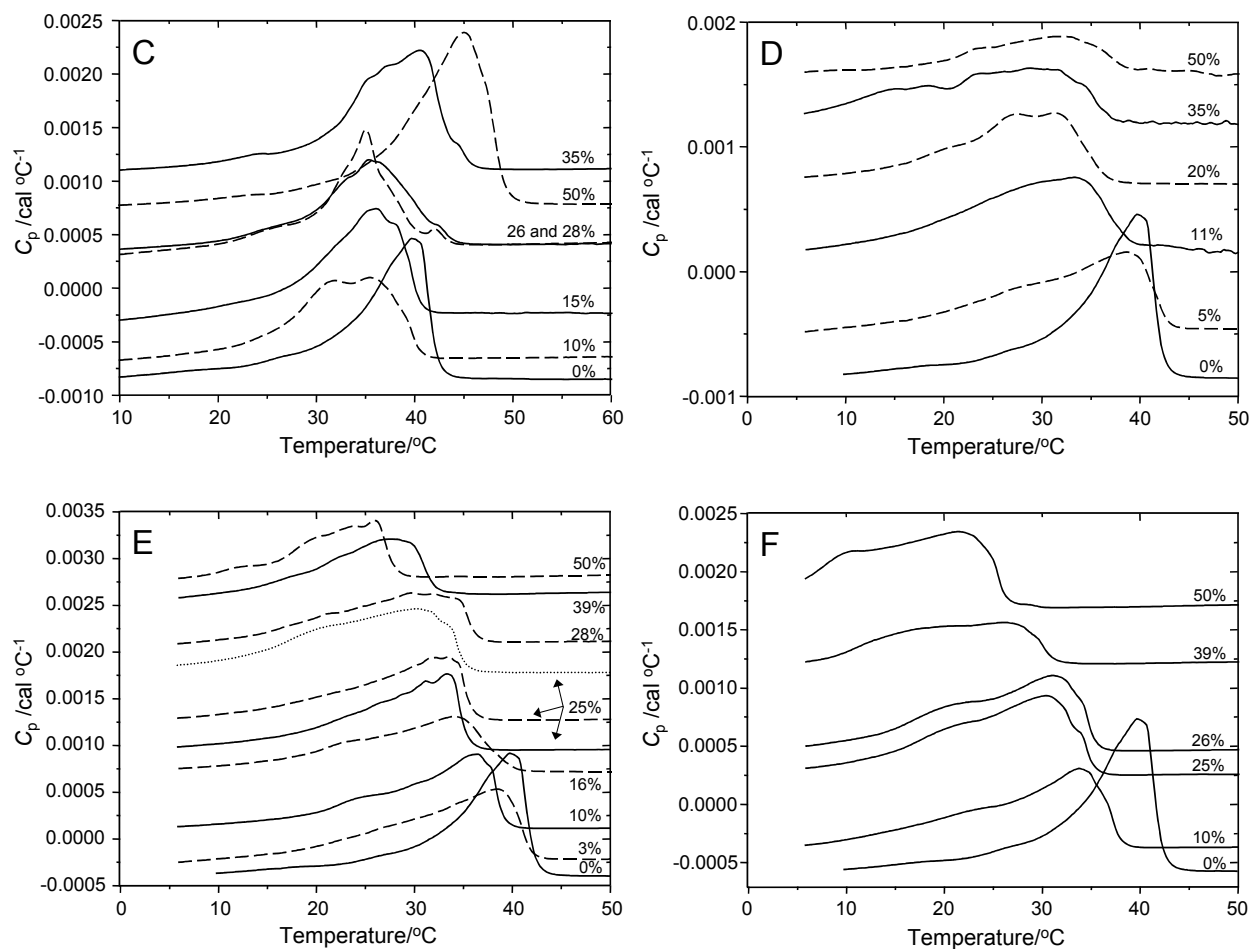


Figure 5. Heating scans for mixtures of $C_{18}C_{18}^+$ and $C_{10}OH$ (A), $C_{18}OH$ (B), $C_{18}GlyOH$ (C), $C_{18:1}OH$ (D), $C_{12}Mal$ (E) and $C_{12}Glu$ (F). The number denotes the mole percentage of alcohol as a function of the total amphiphile concentration. C: the data for 26 mol% is represented by the dashed line. E: dotted line is solution prepared by mixing a vesicular solution of $C_{18}C_{18}^+$ with a micellar solution of $C_{12}Mal$. Lines have been elevated for clarity.

Fluorescence

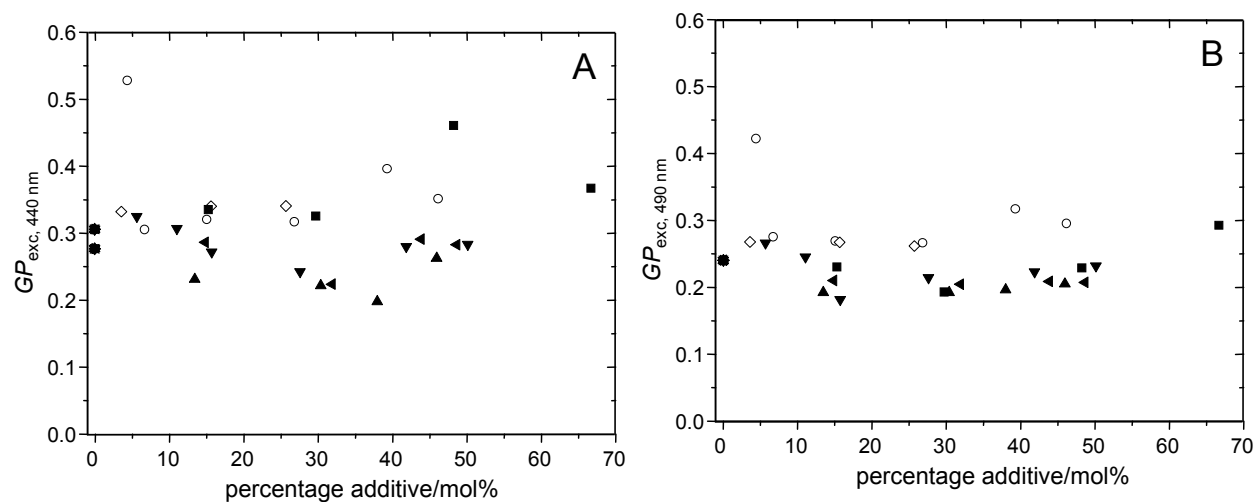


Figure 6. Plots of GP_{exc} versus bilayer composition. Emission followed at (A) 440 nm and (B) 490 nm. $C_{10}OH$ (■); $C_{18}OH$ (▲); $C_{18}GlyOH$ (◄); $C_{18:1}OH$ (▼); $C_{12}Glu$ (○); $C_{12}Mal$ (◇).

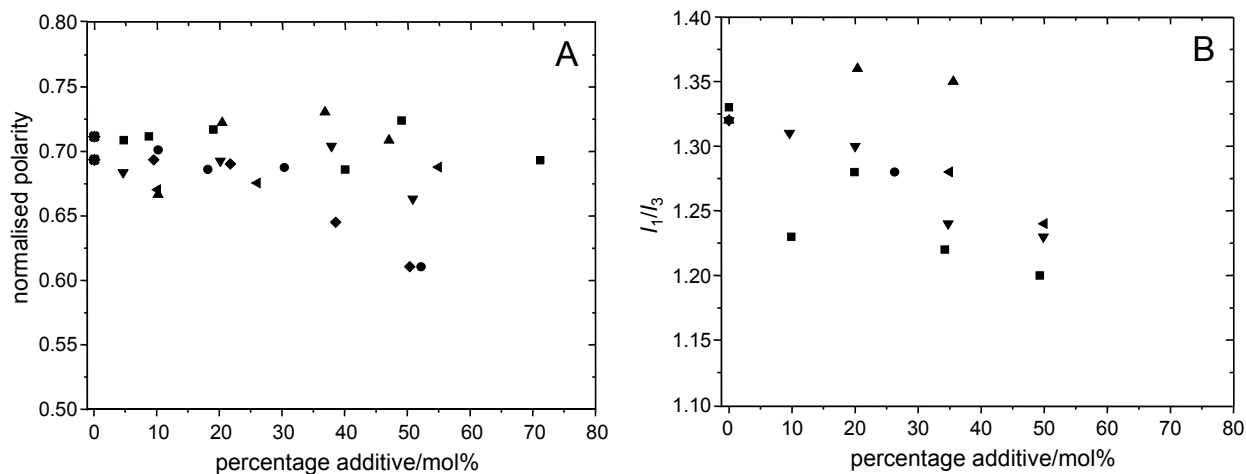


Figure 7. Plots of normalised polarity as sensed by Nile Red excited at 490 nm (A) and I_1/I_3 (B) versus bilayer composition. $C_{10}OH$ (■); $C_{18}OH$ (▲); $C_{18}GlyOH$ (◄); $C_{18:1}OH$ (▼); $C_{12}Glu$ (●); $C_{12}Glu$ (◆).

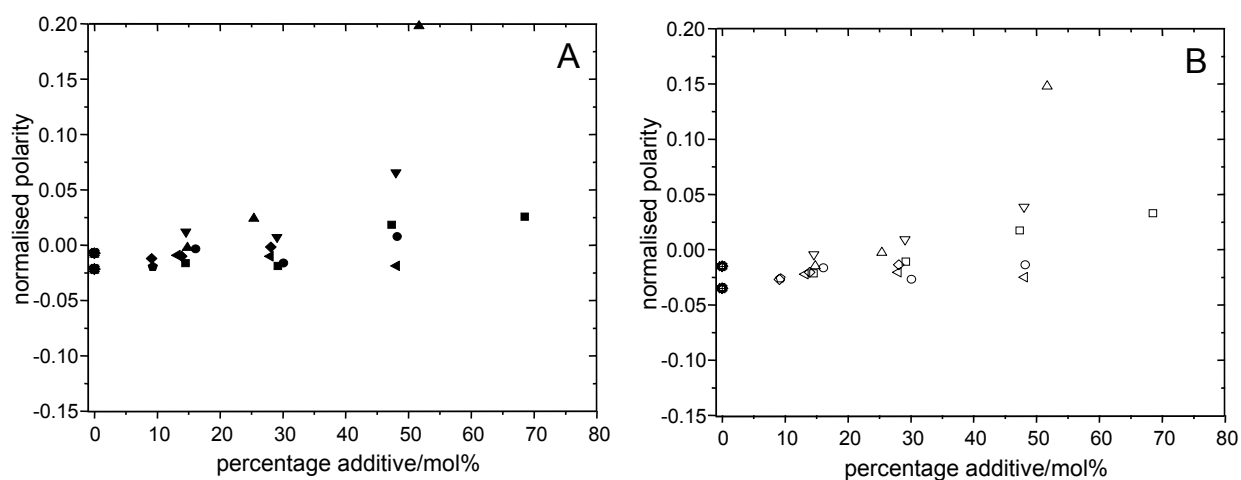


Figure 8. Plots of normalised polarity as measured by ANS versus bilayer composition. A is for solutions without added NaOH, B is for solutions with added NaOH (2.25 mM). $C_{10}OH$ (■); $C_{18}OH$ (▲); $C_{18}GlyOH$ (◄); $C_{18:1}OH$ (▼); $C_{12}Glu$ (●); $C_{12}Mal$ (◆).

References

- (1) K.Ruan, Z.Zhao and J.Ma *Colloid Polym.Sci.* **2001**, *279*, 813-818.
- (2) J.E.Klijn, J.B.F.N.Engberts *J.Am.Chem.Soc.* **2003**, *125*, 1825-1833.
- (3) D.Lichtenberg, R.J.Robson and E.A.Dennis *Biochim.Biophys.Acta* **1983**, *737*, 285-304.

- (4) U.Kragh-Hansen, M.le Maire and J.V.Møller *Biophys.J.* **1998**, *75*, 2932-2946.
- (5) D.Lichtenberg, E.Opatowski and M.M.Kozlov *Biochim.Biophys.Acta* **2000**, *1508*, 1-19.
- (6) M.Johnsson, A.Wagenaar and J.B.F.N.Engberts *J.Am.Chem.Soc.* **2003**, *125*, 757-760.
- (7) M.Johnsson, A.Wagenaar, M.C.A.Stuart and J.B.F.N.Engberts *Langmuir* **2003**, *19*, 4609-4618.